Many-body dynamics of the decay of excitons of different charges in a quantum dot

J. A. Andrade, A. A. Aligia, and Pablo S. Cornaglia
Centro Atómico Bariloche and Instituto Balseiro, Comisión Nacional de Energía Atómica, CONICET, 8400 Bariloche, Argentina
(Received 21 June 2016; revised manuscript received 4 November 2016; published 5 December 2016)

We calculate the photoluminescence spectrum of a single semiconductor quantum dot strongly coupled to a continuum as a function of light frequency, gate voltage, and magnetic field. The spectrum is dominated by the recombination of several excitonic states which can be considered as quantum quenches in which the many-body nature of the system is suddenly changed between initial and final states. This is associated with an Anderson orthogonality catastrophe with a power-law singularity at the threshold. We explain the main features observed experimentally in the region of stability of the trion X^-, the neutral exciton X^0, and the gate-voltage-induced transition between them.

DOI: 10.1103/PhysRevB.94.235109

The optical manipulation of semiconductor quantum dots (QDs) is a subject of great interest because of its potential use to control the electronic spin for quantum information processing [1–3] and spintronics [4–6]. Different optical means of manipulation [6] and detection [5] of the the spin have been proposed. The core of the research in this area consists of optical transitions involving either neutral excitons or trions. These states are respectively bound states of one or two electrons in the conduction band of the QD and a hole in the valence band and can be tuned using a gate voltage, V_g [1–3,7–11].

A ubiquitous aspect of the photoluminescence (PL) decay of excitons of various charges [9–13] or the absorption of light creating them [13–15] is the manifestation of the hybridization of the orbital of the QD with a continuum of extended states. Small QD systems can usually be described by variations of the Anderson impurity model. For small hybridization and an odd number of electrons in the QD, this model reduces to the Kondo model, in which the localized spins have an exchange interaction with the spins of the electrons in the reservoir [9] resulting in a many-body singlet ground state [16].

The PL spectrum that results from the decay of the trion X^- [10,11] and the neutral exciton X^0 [11] has been measured as a function of V_g. The X^- PL line is a consequence of an optical transition to a state with a single electron on average in the QD. As a consequence of the hybridization, the PL is broad near the limits of stability of the trion, it is asymmetric, and there is a nonmonotonic blue shift. While simple approaches were able to explain these features [10,11,17], a fully reliable calculation is still lacking. For the X^0 decay, similar nontrivial effects are present [11]. The creation of the X^0 [15] and X^- [14] states by optical absorption was calculated using the numerical renormalization group (NRG), and in the X^- case there is remarkable agreement with experiment.

These transitions, because of their sudden character, are related to another field of great interest in recent years, the dynamics of highly correlated systems, after a quantum quench [14,15,18–22]. Because initial states (ISs) and final states (FSs) have different local scattering potentials, the spectrum should show at low temperatures a power-law behavior at the PL threshold characteristic of x-ray edge singularities [13–15,23]. This is due to the Anderson orthogonality catastrophe [24], which is another cornerstone of many-body physics and requires sophisticated techniques for its treatment.

An important aspect of the experiment of Kleemans *et al.* [11] is that they worked in the regime of strong hybridization and studied the transition between the X^0 and X^- decays. In this article, we calculate the PL on the whole range of gate voltages, V_g, between the region of stability of X^- and X^0, using NRG within the full-density matrix (FDM) approach [25–29]. Our results provide an explanation of recent experiments and show that a very different behavior of the PL spectrum under an applied magnetic field is expected for the X^0 and X^- decays.

Using Fermi's golden rule, the PL intensity is given by

$$I(\omega) = \frac{2\pi}{\hbar} \sum_{if} w_i |\langle f|H_{LM}|i\rangle|^2 \delta(\hbar\omega + E_f - E_i), \qquad (1)$$

where ω is the PL frequency, $|i\rangle$ labels the IS, $|f\rangle$ denotes the possible FSs, E_j is the energy of the state $|j\rangle$, w_i is the Boltzmann weight of the IS $|i\rangle$, and the relevant part of light-matter interaction can be written as [17]

$$H_{LM} = A(d^\dagger_\uparrow p_{3/2} + d^\dagger_\downarrow p_{-3/2}) + \text{H.c.}, \qquad (2)$$

where $d^\dagger_\sigma$ creates an electron at the QD with spin σ, and p_m annihilates a valence electron with angular momentum 3/2 and projection m [1,30,31]. Equation (1) implies a sudden change in the dynamics of the system equivalent to a quantum quench.

The Hamiltonian is written as

$$\begin{aligned} H = {} & E_e n_d + U_{ee} n_{d\uparrow} n_{d\downarrow} + \sum_{k\sigma} (V_k d^\dagger_\sigma c_{k\sigma} + \text{H.c.}) \\ & + \sum_{k\sigma} \epsilon_k c^\dagger_{k\sigma} c_{k\sigma} + E_h n_h + U_{hh} n_{h3/2} n_{h-3/2} \\ & - U_{eh} n_d n_h + U'_{ee} n_{d\uparrow} n_{d\downarrow} n_h. \end{aligned} \qquad (3)$$

Here $h^\dagger_m \equiv p_m$, $n_{d\sigma} = d^\dagger_\sigma d_\sigma$, $n_{hm} = h^\dagger_m h_m$, $n_d = n_{d\uparrow} + n_{d\downarrow}$, and $n_h = n_{h3/2} + n_{h-3/2}$. The first three terms correspond to the well-known Anderson impurity model. The remaining terms involve heavy holes. The last term takes into account the increase of the repulsion between electrons as their wave function contracts after the addition of holes. Its addition improves the agreement with experiment *simultaneously* for the range of V_g of both the X^- and the biexciton $2X^0$ decay. Contrary to previous approaches, we consider the hybridization in both ISs and FSs. The on-site energies of the QD electrons and holes change with gate voltage as

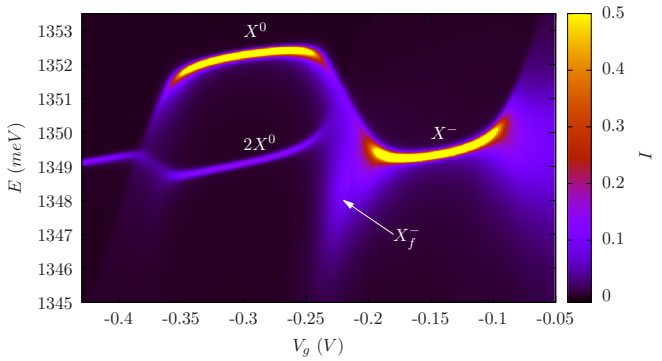

FIG. 1. PL spectrum as a function of gate voltage. The intensity is normalized by twice the maximum intensity at $V_g = -0.35$ V [31]. Parameters are $T = 1.75$ K, $E_e^0 = -25$ meV, $E_h^0 = 1398.5$ meV, $U_{hh} = U_{eh} = U_{ee} + 2U'_{ee} = 20.97$ meV, $U'_{ee} = 3.52$ meV, $\Delta = 1$ meV, and $\lambda = 8$.

$E_e = E_e^0 - eV_g/\lambda$ and $E_h = E_h^0 + eV_g/\lambda$, respectively, where λ is the lever arm [10,11].

Some parameters can be determined by simple features of the experiment [10,11]. For example, neglecting V_k, the amplitude of range of voltage in which the PL spectrum is dominated by the decay of the trion X^- is $V_{ee}^1 = \lambda U_{ee}/e$ (see Fig. 2). We obtain a good agreement with experiment for the parameters indicated in Fig. 1. We assumed the hybridization $\Delta = \pi \sum_k |V_k|^2 \delta(\epsilon_F - \epsilon_k) = 1$ meV independent of energy with support in the range $[-D, D]$, associated with a wide reservoir band of width $2D = 100\Delta$ symmetrically placed around the Fermi energy ϵ_F. There are no particular features of the band or hybridization that can affect the results.

We use the NRG to calculate the PL and compare with the experiments of Kleemans *et al.* [11]. We run the code two times, one in the presence of one or two holes in the valence band of the QD (IS) and the other for one hole less (FS). Then, the density matrix for the ISs and the matrix elements entering Eq. (2) are calculated (see, e.g., Refs. [23] and [14]). In Fig. 1 we show the resulting PL spectrum as a function of V_g. There are two high-intensity plateaus that correspond to the decay of X^0 (lower V_g) and X^- (greater V_g). Near the crossover between them, the plateaus bend and the X^- plateau is joined by another transition line of lower frequency and intensity, which corresponds to that denoted as X_f^- in Ref. [11]. There is another plateau of lower intensity which corresponds to the decay of a biexciton, with two holes and two electrons to the FS X^0. This feature is denoted by $2X^0$ in the experiment [31]. Except for the presence of positively charged Mahan excitons and multiple excitons which involve electron or hole states not included in the Hamiltonian, our results agree with those of Kleemans *et al.* [11].

While the line shape of the PL peaks (discussed below) requires a sophisticated calculation, the evolution of them with V_g and the transition between states of different total charge can be understood qualitatively using a molecular model in which the bandwidth is reduced to a single electron reservoir state with an energy equal to ϵ_F ($D \to 0$) [32]. The most relevant states of this model with less than two holes are represented in Fig. 2. The initial ground state (IGS), before light emission, depending on the value of V_g consists mainly

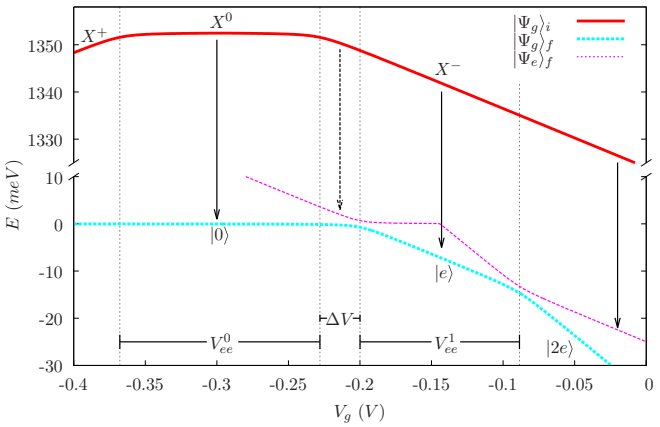

FIG. 2. Most relevant energy levels of the zero-bandwidth model and the PL transitions (indicated with arrows). $|\Psi_g\rangle_i$ and $|\Psi_g\rangle_f$ are the initial and final ground states, respectively. $|\Psi_e\rangle_f$ is an excited FS. Here $V_{ee}^0 = \lambda(U_{ee} + U'_{ee})/e$, $V_{ee}^1 = \lambda U_{ee}/e$, and $\Delta V = \lambda(U_{eh} - U_{ee} - U'_{ee})/e$. The hopping between the QD level and the reservoir effective level is $V = 1$ meV. Other parameters are as in Fig. 1.

of either a single hole (X^+) in the valence band of the QD, or X^0 or X^-, joined by regions with some admixture between X^+ and X^0 or X^0 and X^- due to the hybridization. The FSs after light emission have no hole in the valence band and, similar to the ISs, mainly zero ($|0\rangle$), one ($|e\rangle$), or two electrons ($|2e\rangle$) in the QD. The arrows in Fig. 2 correspond to the main transition in each voltage regime. The feature denoted as X_f^- corresponds to the transition, indicated by a dashed arrow, from the trion to an excited state with a dot occupancy between zero and one. The observed plateaus in the PL spectrum can be understood in the $V = 0$ limit. The transition $X^0 \to |0\rangle$ takes place, with an emission energy of $\hbar\omega = E_e^0 + E_h^0 - U_{eh}$, in the interval $E_e^0 - U_{eh} \leqslant eV_g/\lambda \leqslant E_e^0 - U_{eh} + U_{ee} + U'_{ee}$. The high V_g plateau in Fig. 1, with an energy of $E_e^0 + E_h^0 - 2U_{eh} + U_{ee} + U'_{ee}$, stems from the electron-hole recombination of the trion $X^- \to |e\rangle$, in the range $E_e^0 \leqslant eV_g/\lambda \leqslant E_e^0 + U_{ee}$.

When the hybridization is turned on, both the IS and FS energies decrease by $\sim\Delta$. These energy gains calculated with NRG-FDM and their difference, which gives the shift in PL frequency, are represented in Fig. 3. As expected, the energy gain is larger near the intermediate valence regions. For example, there is a dip in the energy of the FS at $V_g = \lambda E_e^0/e = -0.2$ V for which the occupancy of the FS at the dot n_d is intermediate between 0 and 1. Another dip is clear for $V_g = \lambda(E_e^0 + U_{ee})/e = -0.088$ V for which $n_d \approx 1.5$. Note that even in the Kondo regime $V_g \approx -0.144$ V, for which $n_d \approx 1$, the energy gain is of the order of Δ in contrast to expectations from simple approaches [11,17]. For $V_g \geqslant \lambda E_e^0/e$, the net effect of the hybridization is a blue shift which is more pronounced for intermediate valence occupancy of the FSs. Similarly, in the region of the X^0 decay, the effect of the hybridization is a red shift, larger near the limits of stability of X^0 against either X^+ or X^-. These shifts explain characteristic features of the PL frequency as a function of the gate voltage V_g observed in the experiment and reproduced in Fig. 1, in particular, the downward curvature in the X^0 region and an upward curvature in the X^- region. A similar

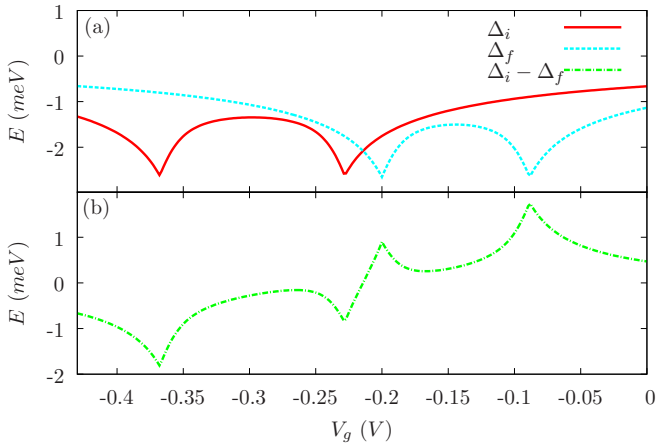

FIG. 3. (a) Green solid line: Energy gain Δ_i of the IS before photoemission due to hybridization. Blue dashed line: Energy gain Δ_f for the FS after photoemission. (b) Change of the emitted photon energy gain $\Delta_i - \Delta_f$ due to hybridization.

reasoning can be followed for the $2X^0$ feature leading to the same qualitative behavior as for the X^- decay, in agreement with the results shown in Fig. 1.

In Fig. 4 we show two PL line shapes that correspond to the X^0 decay for $V_g = -0.35$ and -0.3 V and the respective experimental results digitized from Ref. [11]. The comparison is excellent. The long tails at low energies provide evidence of the excitations produced by the sudden change of the dynamics of the system (quantum quench) associated with an Anderson orthogonality catastrophe. To discuss this point in more detail, in Fig. 5 we show the PL intensity shift from the threshold ω_e^* in a logarithmic scale, for temperatures much smaller than the Kondo temperature T_K and three values of the gate voltage: $V_g = -0.144$ V corresponding to the Kondo regime for the FS in the X^- decay; $V_g = -0.214$ V in the region between the X^0 and X^- decays, where the PL frequency changes strongly as a function of gate voltage and both ISs and FSs are in the intermediate-valence regime; and last,

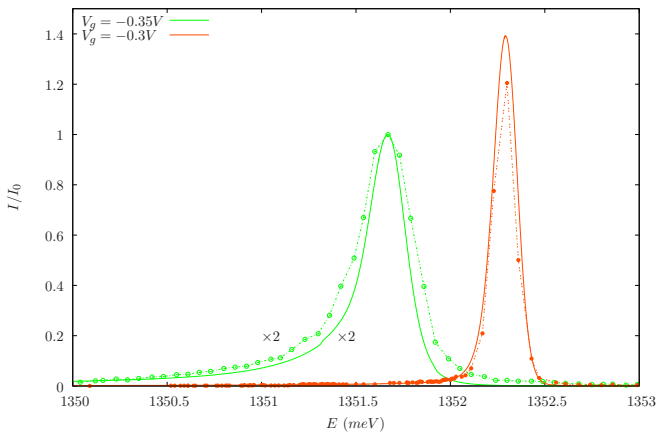

FIG. 4. PL intensity close to the onset of the X^0 plateau (green solid line) and at the center of the X^0 plateau (orange solid line). The orange solid and green open circles are the corresponding digitized results of Kleemans *et al.* [11]. $I_0 = I(1351.6$ meV) for $V_g = -0.35$ V.

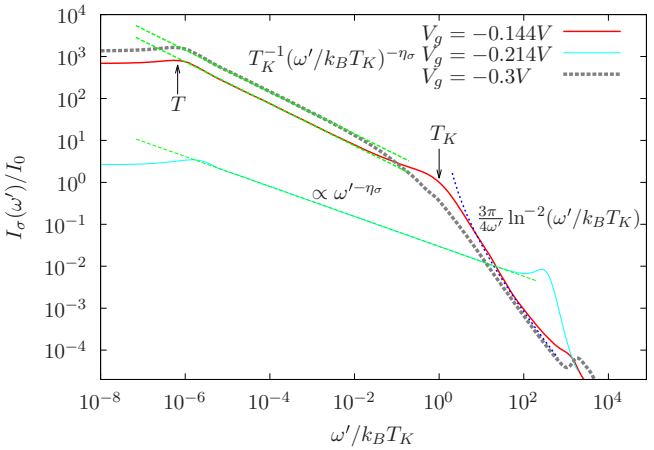

FIG. 5. PL intensity as a function of the frequency $\omega' = \omega_e^* - \omega$ shift from the threshold (ω_e^*) in a log-log scale for three values of the gate voltage, -0.144, -0.214, and 0.3 V. The thresholds are 1349.74, 1350.34, and 1352.54 meV, respectively. The intensity is normalized by $I_0 = I(k_BT_K/\hbar)$ calculated for $V_g = -0.144$ V, where $T_K \sim 0.083$ K.

$V_g = -0.3$ V corresponding to the Kondo regime for the IS in the X^0 decay. In the first case, as the frequency is lowered, we recover the same regimes studied theoretically before for absorption of light creating X^0 [15]. At high frequency, the physics is dominated by the free-orbital fixed point of the NRG, with a dependence $I(\omega) \sim \omega^2$. Lowering the frequency the functional form turns to that of the local moment fixed point until the Kondo frequency $k_BT_K/\hbar$ is reached. For $\hbar\omega < k_BT_K$, the physics enters the strong-coupling regime, and the dependence is the characteristic power law $\omega^{-\eta_\sigma}$ for the Anderson orthogonality catastrophe associated with the quantum quench in a Fermi liquid. The exponent is given by $\eta_\sigma = 1 - \sum_{\sigma'}(\delta_{\sigma\sigma'} - \Delta n_{\sigma'})^2$ [15], where $\Delta n_{\sigma'}$ is the change on the local occupation of electrons with spin projection σ', between the FS and IS. This divergent behavior at low frequency ceases at a frequency $k_BT/\hbar$ determined by the temperature. For $V_g = -0.214$ V, the behavior is similar, except for the absence of the local moment regime and the different exponent η_σ. For $V_g = -0.3$ V (X^0 decay), the local moment regime cannot be reached and the PL intensity is about four times smaller at $\omega \sim k_BT_K/\hbar$ than for the X^- decay. The result is a smoother curve, similar to light absorption leading to X^- [14].

From the occupancies of the different states, we obtain $\eta_\sigma = 0.4987$ for $V_g = -0.144$ V, $\eta_\sigma = 0.3571$ for $V_g = -0.214$ V, and $\eta_\sigma = 0.4983$ for $V_g = -0.3$ V The corresponding curves $\omega^{-\eta_\sigma}$ are also represented in Fig. 5 with the intensity as the only fitting parameter.

Finally, we analyze the effect of an external magnetic field B (see Fig. 6),[1] which leads to a splitting of the PL plateaus due to the different giromagnetic factors for electrons and holes [14]. The different broadening of the PL peaks is due to the B dependence of η_σ (see Fig. 7) [15]. Plateaus associated with the recombination of a spin down electron

[1]Following Ref. [14] we take the giromagnetic factors of the hole and the electron as $g_h = 1.1$ and $g_e = -0.6$, respectively.

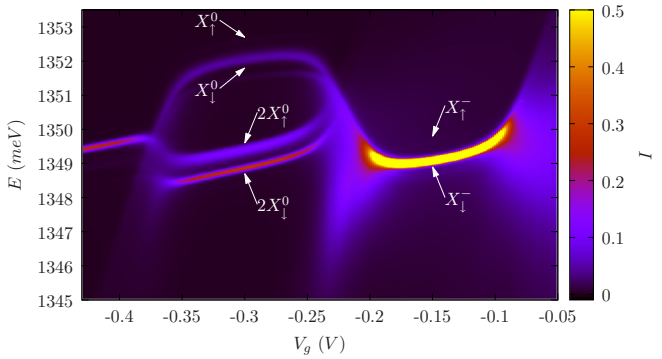

FIG. 6. PL intensity in the presence of an external magnetic field producing a Zeeman splitting 0.57 meV of the electronic level of the QD and an ∼1.05 meV splitting for the hole level at $T = 1.75$ K.

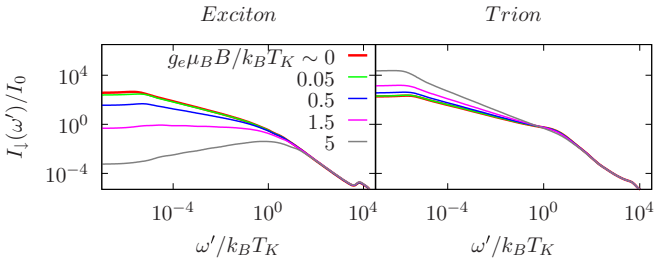

FIG. 7. PL intensity as a function of the frequency shift from the threshold for different values of the magnetic field. The left side panel is in the exciton decay regime ($V_g = -0.3$ V) and the right side panel is for trion decay ($V_g = -0.144$ V). The PL intensity for the spin up projection $I_\uparrow(\omega)$ (not shown) is exponentially suppressed for $g_h\mu_B B > k_B T$. Other parameters are as in Fig. 5.

have an exponentially suppressed intensity for the $X^0_\downarrow$ and $X^-_\downarrow$ decays at low temperatures which is mainly due to the reduced probability of finding a hole with a high energy spin projection in the IGS. For the $2X^0$ decay the electron and hole spins are compensated in the IGS and the $2X^0_\uparrow$ and $2X^0_\downarrow$ plateaus have a sizable intensity and are clearly visible in the figure.

In summary, using an Anderson impurity model, we can explain experimental results of PL in a wide range of gate voltages, including those for which either ISs or FSs or both are in the mixed valence regime. The PL transition is an experimental realization of a quantum quench associated with another realization of Anderson orthogonality catastrophe, but in contrast to previous studies, in our system electron correlations are important in both ISs and FSs in the photon decay. We find a marked asymmetry in the PL line shapes for the neutral exciton and trion decays both in the hybridization-induced energy shift and in the dependence on the magnetic field. Absorption and emission of light are qualitatively different and the local moment regime can be reached only in the FS (X^0 absorption or X^- decay).

We are supported by CONICET. This work was sponsored by Grant No. PIP 112-201101-00832 of CONICET and Grant No. PICT 2013-1045 of the ANPCyT.

[1] M. Atatüre, J. Dreiser, A. Badolato, A. Högele, K. Karrai, and A. Imamoglu, Science **312**, 551 (2006).
[2] A. Greilich, R. Oulton, E. A. Zhukov, I. A. Yugova, D. R. Yakovlev, M. Bayer, A. Shabaev, Al. L. Efros, I. A. Merkulov, V. Stavarache, D. Reuter, and A. Wieck, Phys. Rev. Lett. **96**, 227401 (2006).
[3] J. Berezovsky, M. H. Mikkelsen, N. G. Stoltz, L. A. Coldren, and D. D. Awschalom, Science **320**, 349 (2008).
[4] S. Mackowski, T. Gurung, H. E. Jackson, L. M. Smith, G. Karczewski, and J. Kossut, Appl. Phys. Lett. **87**, 072502 (2005).
[5] M. Korkusinski and P. Hawrylak, Phys. Rev. Lett. **101**, 027205 (2008).
[6] D. E. Reiter, T. Kuhn, and V. M. Axt, Phys. Rev. Lett. **102**, 177403 (2009).
[7] R. J. Warburton, C. Schöflein, D. Haft, F. Bickel, A. Lorke1, K. Karrai, J. M. Garcia, W. Schoenfeld, and P. M. Petroff, Nature (London) **405**, 926 (2000).
[8] A. Högele, S. Seidl, M. Kroner, K. Karrai, R. J. Warburton, B. D. Gerardot, and P. M. Petroff, Phys. Rev. Lett. **93**, 217401 (2004).
[9] J. M. Smith, P. A. Dalgarno, R. J. Warburton, A. O. Govorov, K. Karrai, B. D. Gerardot, and P. M. Petroff, Phys. Rev. Lett. **94**, 197402 (2005).
[10] P. A. Dalgarno, M. Ediger, B. D. Gerardot, J. M. Smith, S. Seidl, M. Kroner, K. Karrai, P. M. Petroff, A. O. Govorov, and R. J. Warburton, Phys. Rev. Lett. **100**, 176801 (2008).
[11] N. A. J. M. Kleemans, J. van Bree, A. O. Govorov, J. G. Keizer, G. J. Hamhuis, R. Nötzel, A. Yu. Silov, and P. M. Koenraad, Nat. Phys. **6**, 534 (2010).
[12] S. Cao, J. Tang, Y. Sun, K. Peng, Y. Gao, Y. Zhao, C. Qian, S. Sun, H. Ali, Y. Shao, S. Wu, F. Song, D. A. Williams, W. Sheng, K. Jin, and X. Xu, Nano Res. **9**, 306 (2016).
[13] R. W. Helmes, M. Sindel, L. Borda, and J. von Delft, Phys. Rev. B **72**, 125301 (2005).
[14] C. Latta, F. Haupt, M. Hanl, A. Weichselbaum, M. Claassen, W. Wuester, P. Fallahi, S. Faelt, L. Glazman, J. von Delft, H. E. Türeci, and A. Imamoglu, Nature (London) **474**, 627 (2011).
[15] H. E. Türeci, M. Hanl, M. Claassen, A. Weichselbaum, T. Hecht, B. Braunecker, A. Govorov, L. Glazman, A. Imamoglu, and J. von Delft, Phys. Rev. Lett. **106**, 107402 (2011).
[16] A. C. Hewson, in *The Kondo Problem to Heavy Fermions* (Cambridge University Press, Cambridge, England, 1993).
[17] L. M. León Hilario and A. A. Aligia, Phys. Rev. Lett. **103**, 156802 (2009).
[18] P. Nordlander, M. Pustilnik, Y. Meir, N. S. Wingreen, and D. C. Langreth, Phys. Rev. Lett. **83**, 808 (1999).
[19] M. Heyl and S. Kehrein, Phys. Rev. Lett. **108**, 190601 (2012).
[20] R. Vasseur, K. Trinh, S. Haas, and H. Saleur, Phys. Rev. Lett. **110**, 240601 (2013).
[21] S. L. Lukyanov, H. Saleur, J. L. Jacobsen, and R. Vasseur, Phys. Rev. Lett. **114**, 080601 (2015).
[22] A. E. Antipov, Q. Dong, and E. Gull, Phys. Rev. Lett. **116**, 036801 (2016).
[23] P. S. Cornaglia and A. Georges, Phys. Rev. B **75**, 115112 (2007).
[24] P. W. Anderson, Phys. Rev. Lett. **18**, 1049 (1967).

[25] K. G. Wilson, Rev. Mod. Phys. **47**, 773 (1975).
[26] R. Bulla, T. A. Costi, and T. Pruschke, Rev. Mod. Phys. **80**, 395 (2008).
[27] M. Yoshida, M. A. Whitaker, and L. N. Oliveira, Phys. Rev. B **41**, 9403 (1990).
[28] A. Weichselbaum and J. von Delft, Phys. Rev. Lett. **99**, 076402 (2007).
[29] W. C. Oliveira and L. N. Oliveira, Phys. Rev. B **49**, 11986 (1994).
[30] In principle, Eq. (2) contains another term in which $d_\sigma^\dagger$ is replaced by band electrons [11]. However this term is small and we have verified that it does not modify substantially our results.
[31] To take into account the smaller probability of excitations of two holes in the experiment, we have multiplied the weight of the initial states with two holes by 0.1 with respect to those with one hole.
[32] This molecular model is similar to the zero bandwidth model described in the supplementary information of Ref. [11] but we include all charge configurations.